DEVELOPMENT OF EXPERIMENTAL SMALL UAV EQUIPPED WITH CELLULAR PHONE DATA LINK SYSTEM

Daisuke Kubo*, Shinji Suzuki, Takaaki Kagami*****
***Doctoral student, Department of Aeronautics and Astronautics, The University of Tokyo**
****Professor, Department of Aeronautics and Astronautics, The University of Tokyo**
*****Solekia Limited**

Keywords: *Unmanned Aerial Vehicles, Aircraft Design, Data Link System, Environmental Monitoring*

Abstract

Experimental small Unmanned Aerial Vehicles (UAVs), OBK-SkyEye family were developed to explore the feasibility and utility of small, 'one-person-portable', UAVs in this project. These vehicles were no more than 1.5 m in the wingspans and 1.5 kg in the weights. SkyEye2 flies autonomously using a micro autopilot system. Video images from an onboard camera and telemetry signals from the autopilot were sent to a Ground Control Station (GCS) and command signals were sent to the vehicle using a developed cellular phone data link system, successfully. Successor vehicle SkyEye3 demonstrated in environmental monitoring flights over forest area, collaborating with a forestry research center. A visible/near-IR digital camera unit modified from commercial compact digital cameras was used in the flights. Collected data were processed into false-color images and orthomosaic images useful for analysis of the forest area.

1 Introduction

Unmanned aerial vehicles (UAVs) have been playing important roles in military missions [1]. Furthermore, civil missions are increasing for reconnaissance in hazardous districts, rescue activities, meteorological monitoring and so on. There are various configurations, sizes and complexities of systems. Considering practical operations in civil airspace, the UAVs should be equipped with highly sophisticated autonomous flight capabilities. Since such systems are often too large and heavy to install in small airframes, UAVs with large airframe are needed to install them. Therefore, it may be possible to operate only Global Hawk [2] or Altair [3] in civil airspace under the present circumstances. However large UAVs involve a considerable operational cost and many infrastructures like long paved runways. On the other hand, small UAVs are also candidates for civilian use because they have advantages with regard to operational costs, human resources, and readiness. These advantages are more important in civil use than in military use. Furthermore, small UAVs can be used in special missions such as high-resolution aerial photography from low altitude, which larger UAVs cannot accomplish. The rapid development of small sensors using micro-electro-mechanical systems (MEMS) and microprocessors make it possible to design small UAVs, and some of them have been demonstrated in civil missions [4][5].

The Innovative Aerial Robot Project (IARP) team in the University of Tokyo develops an experimental small UAV, OBK-SkyEye family in cooperation with industries. SkyEye1 is a conceptual model, SkyEye2 is an experimental model [6] and SkyEye3 is a demonstration model. These vehicles were no more than 1.5m in the wingspans and 1.5 kg in the weights, which make them 'one-person-portable'.

When UAVs are operated in civil missions, there are additional issues of radio communications between vehicles and ground control station (GCS), because useable radio frequency and emission power are limited by

laws in each country. The lawful emission power of allowed radio frequency isn't high enough to reach desired distance for UAV systems, in the case of Japan. In this study, a data link system equipped with cellular phone cards was demonstrated with OBK-SkyEye2. The communication system can link them, as long as the vehicle flies anywhere in the service area of the cellular phones.

The successor OBK-SkyEye3 was demonstrated in aerial observation missions at forest area collaborating with Hiroshima prefectural forestry research center, Japan. The results are shown in this paper.

2 Vehicle Design

2.1 Design Requirements

The experimental UAV had the following two missions.

1) Flight data logging with an autopilot to evaluate developed vehicle performances
2) Experimenting autonomous flight and communication using cellular phone line

The first mission requires that a plane can fly at low speed in a compact area. The baseball ground in our university campus as shown in Fig.1 was selected as a flight test field. In order to perform "figure of 8" flights, the minimum turn radius should be no more than 12.5 m. This turn radius had to be achieved with a reasonable bank angle ϕ and lift coefficient C_L.

The second mission determines the weight and size of payloads. Since all of payloads including an autopilot and cellular phone data link system are mounted in a fuselage, the size of the fuselage is specified.

2.2 Basic Configuration

For the first mission, only the autopilot MicroPilot Inc. MP2028g and its accessory equipments were considered as payloads, thus the total weight of the payloads was assumed to be no more than 250 g, including a 50 g margin. Necessary space for payloads was measured for the communication unit.

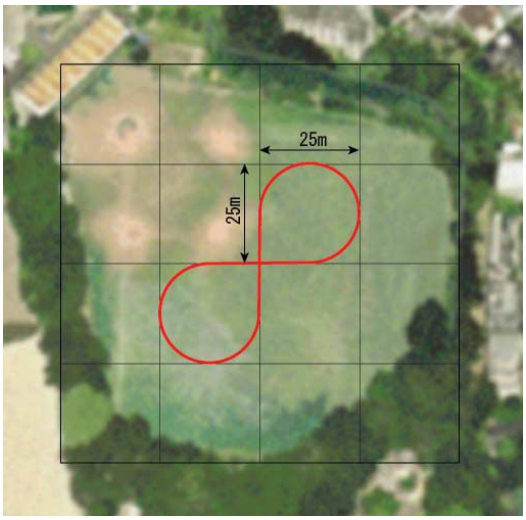

Fig. 1 Test Flight Filed

The choice of a power plant is one of the most important processes in preliminary design. A DC brushless motor with a Lithium-polymer (Li-Po) battery was selected as a power unit. Rapid developments of the DC brushless motors, their drive controllers using MOSFET technology and Li-Po batteries make it possible to develop small electric UAVs with practical flight performances. Electric motors have many advantages over model gasoline engine, for example convenience in operations, low vibration level, high reliability and no-pollution emission into environment. These characteristics are very useful in practical operations, especially in civil missions.

The original configuration was determined as follows:

1) High Wing Configuration: The strong stability characteristics are desirable for both human and developing autopilot operations.
2) No Ailerons: In some cases, ailerons are not effective at low speed or high lift coefficient flight sine the aileron deflection may cause an unsymmetrical stall. The vehicle was equipped only with a rudder for lateral control without ailerons.
3) Tractor arrangement: A conventional tractor type layout for engine position is selected since it is desirable for stability characteristics.

2.3 Sizing Process

The conventional sizing process illustrated in Fig.2 determines the size of an airframe. First, a takeoff weight W_{TO} was assumed. A wing area was estimated by using the specified wing loading (W_{TO}/S), which was derived from

$$\frac{W}{S} = \frac{1}{2}\rho g r C_L \sin\phi \qquad (1)$$

where the turn radius was defined as 12.5 m and the bank angle ϕ and the lift coefficient C_L was assumed as 30 deg and 0.65 respectively. Second, assuming appropriate tail volumes, the tail wing and fin areas were obtained. Third, motor, propeller, and battery were selected. In this selection, we utilized the software CEMAP (Calculation script of an Electric Model AirPlane) [7], which contained the motor models, battery models, and propeller models to evaluate battery-motor-propeller matching. Finally, weights of all components were estimated based on statistical data of model airplanes. If the estimated take-off weight was different from the initial guess, the above process was repeated until the take-off weight converged.

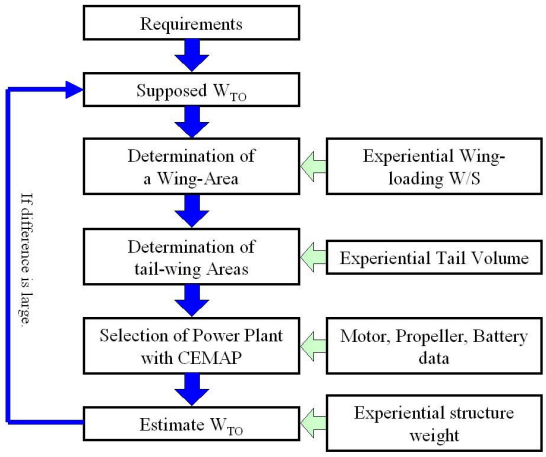

Fig. 2 Flow Chart of Sizing Process

2.4 Drawing

Figure 3 is the three views of the designed vehicle. Note that it has a big fuselage for payloads and the designed take-off weight of 850 g (initial). The airfoil of the main wing is Clark-Y airfoil, which has a flat bottom surface and is often used for model planes. A tail wing and a vertical fin have a flat surface airfoil.

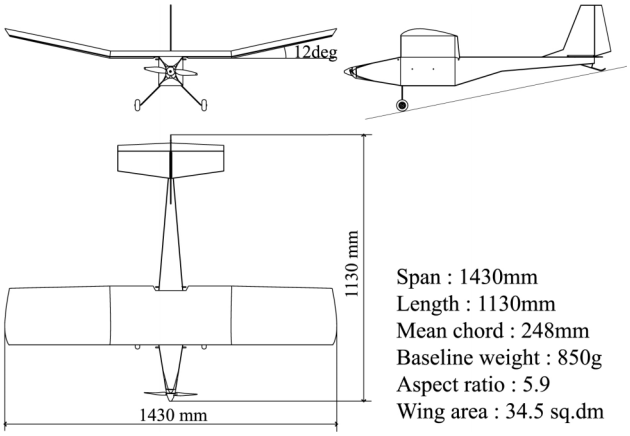

Fig. 3 Three Views of Designed Vehicle

3 Mathematical Modeling and Simulation

3.1 Inertia Characteristics

In addition to the take-off weight, the inertia data such as the inertia moment must be evaluated for flight simulations. A 3-dimentional (3D) computer aided design system (CAD) model, shown in Fig.4, was prepared to calculate the center of the gravity and the inertia matrix.

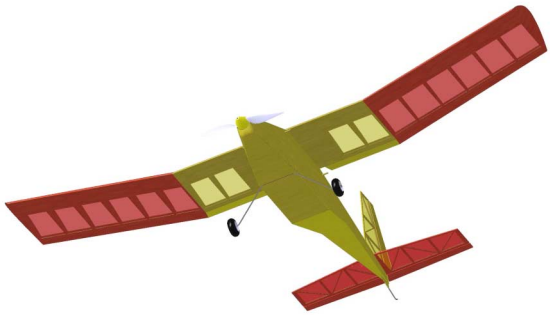

Fig. 4 Three-Dimensional CAD model

3.2 Aerodynamic Characteristic

Aerodynamic Characteristics and stability derivatives were estimated using a simple method described in classical textbooks. Those data were confirmed by wind tunnel tests. A 70 % scale model without propulsion was constructed for the tests as shown in Fig.5. A low speed wind tunnel facility with a Goettingen-type with open rectangular 1.0 by 1.5 m test section was used. The tested angles of attack α range was from −12 to +24 deg and sideslip angles β range was from 0 to +30 deg, symmetry of the airframe was assumed. The Reynolds number of the test was $Re = 1.4\times10^5$. All derived results of this paper were corrected using wind tunnel boundary correction method [8].

Fig. 5 70% Scale Model for Wind Tunnel Testing

Figure 6 shows one of the derived data, lift, drag, and moment coefficients, which show

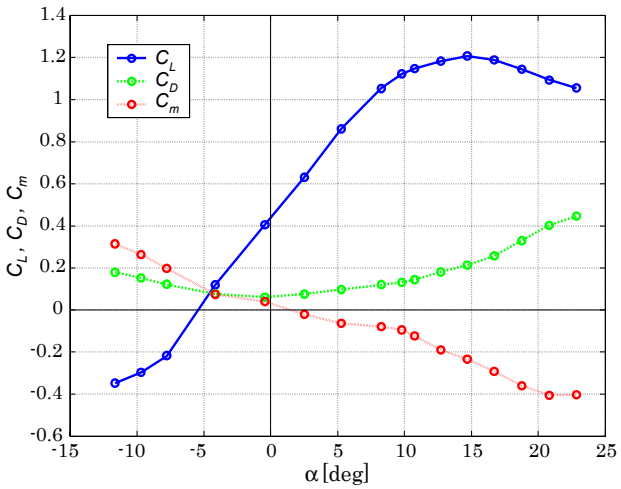

Fig. 6 Aerodynamic Characteristics Measured in Wind Tunnel Testing

mild stall characteristics. Using these data, stability derivatives were obtained and illustrated in Table 1 with estimated ones. They showed a reasonable agreement between estimated and measured ones. Therefore, it is concluded that classical estimation methods are useful for this class of small UAVs.

Table 1 Stability Derivatives

Derivatives	Experiments	Predicts
C_{x_α}	0.377	0.260
C_{z_α}	-4.217	-4.639
C_{L_α}	4.134	4.639
C_{m_α}	-0.767	-0.557
$C_{z_{\delta_e}}$	-0.204	-0.264
$C_{m_{\delta_e}}$	-0.587	-0.708
C_{y_β}	-0.727	-0.285
C_{l_β}	-0.154	-0.222
C_{n_β}	0.149	0.122
$C_{y_{\delta_r}}$	0.125	0.157
$C_{l_{\delta_r}}$	0.007	0.011
$C_{n_{\delta_r}}$	-0.068	-0.071

3.3 Propulsion Model

Propeller characteristics were calculated using momentum blade element theory [9]. Thrust coefficient C_T and power coefficient C_p were derived as functions of advance ratio J. DC electric motor model was used to calculate torque from revolution speed and input voltage (throttle settings).

3.4 Flight Simulation

To evaluate flight characteristics, 6-degree of freedom (DOF) nonlinear dynamic equations were solved numerically using Simulink and AeroSim Blockset [10]. The maneuver capability with a small turn radius and stable flight characteristics were indicated through the simulations.

4 Vehicle Construction and Test Flights

The constructed vehicle is illustrated in Fig.7 Almost all of the structures are made with balsa woods and some concentric loaded structures such as motor mount and landing gears mount are made with plywood. The surface is covered with thin polyester films, which reinforce the structures by their tensions.

Fig. 7 Constructed OBK-SkyEye2

The weight distribution in this step is summarized in Table 2. It should be mentioned that a payload capacity was reduced to 213 g from 250 g. It is because that reinforcing parts like plywood for landing gear mount is much heavier than estimated. However, 50 g of margin weigh was considered in the estimated payload, and the difference did not cause any problems.

Table 2 Weight Distribution

Main wing	145.8 g
Fuselage and gears	199.2 g
Horizontal tail wing	20.0 g
Vertical fin	11.7 g
Motor, amp and receiver	111.9 g
Propeller and spinner	30.0 g
Battery	115.6 g
Others	2.9 g
Payload	212.9 g
Total Take off weight	850.0 g

Test flights were carried out at the baseball ground on the university campus. Flight data were recorded using installed MP2028g autopilot. The recorded data indicated that the turn radius was from 20 m to 30 m. It can be said that the requirement for turn performance was satisfied.

Since the propulsion unit has some power margin, the vehicle has a potential to fly with heavier payload if there is no flight area constraint. In the autonomous flight test phase to be described below, the flight test field was changed to a larger space, the requirement on the turn radius was relaxed and the maximum payload became 500 g experimentally. So, all equipments including cellular phone data link system were able to be installed without any problem.

5 System Configuration

The OBK-SkyEye system configuration is illustrated in Fig.8. A pilot usually launch the vehicle using a radio control (RC) transmitter and change to autonomous mode using a switch on the transmitter after reaching a safe altitude, typically 30 m above the ground. Then the vehicle autonomously flies to waypoints (WPs) in turn. Another operator can monitors status of the vehicle and command flight plan change like positions of WPs using a ground control station (GCS) laptop. The pilot usually flies the vehicle in landing phase. If the operation fields are flat enough, autonomous take-off and landing are also available with an ultrasonic above ground level (AGL) sensor.

Two slot-in type cellular phone cards that

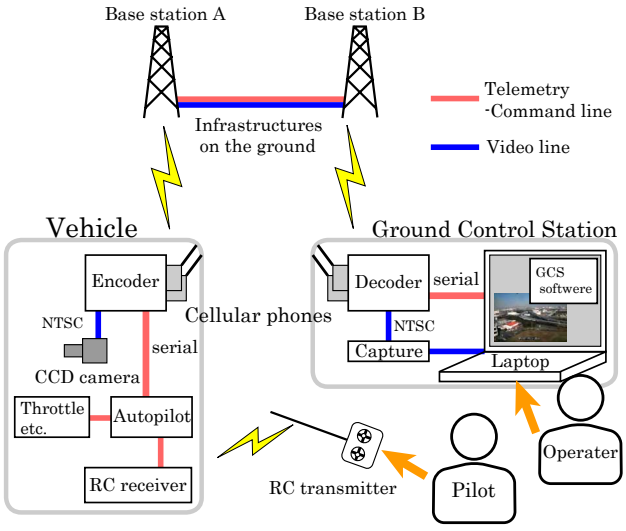

Fig. 8 Data Link System Configuration

are usually used as wireless network connection devices for laptops were used in an encoder for vehicles and a decoder on GCS respectively. The devices are shown in Fig.9.

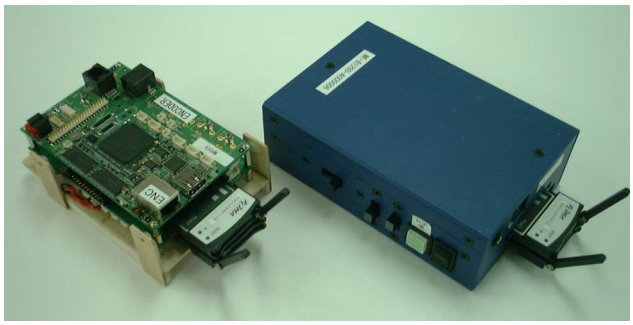

Fig. 9 Encoder and Decoder Equipped with Cellular Phone Cards

Video data from the onboard camera are compressed with the onboard encoder. Then, the compressed data go to the decoder at the decoder on GCS through cellular phone communication ground infrastructures. The decoded outputs, national television standards committee (NTSC) video composite signals, are captured using analog video capture device connected to the GCS laptop and displayed. The data link devices weren't originally developed for this project. Pre-developed ones were utilized with some modifications to demonstrate the system with a limited cost. So, final output on the laptop display doesn't have the ideal quality, because data format are converted between digital and analog multiple times through the data streamline.

The telemetry data such as vehicle position, attitude and status are sent from the autopilot to the GCS decoder through the cellular phone communication line together with the video data. Then the decoded signals are sent to a GCS application on the laptop through a virtual serial port. The command data are sent reversely.

6 Flight Tests

6.1 Autonomous Flight Tests

Global Positioning Systems (GPS) combined with MEMS sensors can realize low-cost and compact autonomous flight control system for small UAVs. As an autonomous flight control system, MicroPilot Inc. MP2028g was selected. It has 3 axis accelerometers, 3 axis gyros, and pilot tubes as sensors. Integrating these sensors with GPS, the system has the ability to hold an altitude and navigate to pre-programmed coordinates, what is called waypoints (WPs). After some flight tests to adjust feedback gains of the PID controller, autonomous flights targeting waypoints were carried out successfully.

6.2 Data Communication Tests

The third generation (3G) cellular phones were utilized to interface with the autopilot system. The cellular phones were also used for transmitting video data captured from a UAV. Although the communication speed of the cellular phone system was not enough, it could cover a wide range where cellular phones were available. First, video transmission was tested in flight. Fig.10 shows the video image transmitted using cellular phones.

Fig. 10 Video Image Transmitted Using Cellular Phone Data Link System

6.3 Whole System Demonstrations

In-flight tests of telemetry and command line communication were carried out after ground tests. After solving some problems, such as electromagnetic interference and the position of an antenna, the communication was carried out successfully. Fig.11 illustrates the result in

which waypoint WP2 was changed to WP3 using communication command during the flight and the UAV were able to change flight paths autonomously.

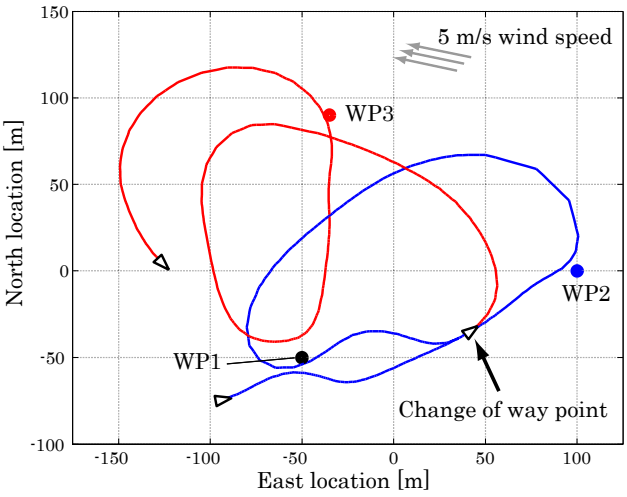

Fig. 11 Change of Waypoint

7 Application to Aerial Observation Missions

Hiroshima prefectural forestry research center had been researching into plants distribution of Yahata moor using balloon aerial photography. Yahata moor is located about 700 m above the sea level. The observation target area of Yahata moor is 600 m length from east to west and 900 m length from north to south. Almost all over the area are covered with trees and low bush. There is an almost straight paved road west side of the area. The research center has been trying to recover the natural condition, which was destroyed by human activities. The balloons they had been using in the photography have a disadvantage of displacement difficulty in forests and are sensitive to gusts. So, small UAVs were selected as candidate of observation platforms.

7.1 Instruments

OBK-SkyEye3 shown in Fig.12, which is the successor vehicle of SkyEye2 was used. Radio modems using 2.4 GHz frequencies with low emission power were used in this mission, because of payload weight limitation. Sensor payload was a visible/near-infrared (IR) multi-bands digital camera unit, shown in Fig. 13, including two commercial compact digital cameras; one was with normal visible capability and another was modified with near-IR capability. They can synchronously and automatically release their shutters, at interval of 4 seconds using interval timer unit controlled from the autopilot in flight.

Fig. 12 Successor OBK-SkyEye3

Fig. 13 Multi Bands Digital Camera

7.2 False-Color Images

The visible and near-IR images collected with the cameras were processed into false-color composite images. One of the results is shown in Fig.14. Near-IR band from near-IR camera, and red band and green band from visible camera were coded respectively as red, green and blue (RGB) components of false-color images.

Since chlorophylls in plants reflect near-IR strongly, bright red and pink color in this image shows the chlorophylls. Since water and asphalt reflect little near-IR, there is little red color component on them. Such images are useful in analyzing distributions and variations of plants or damages of forest fires.

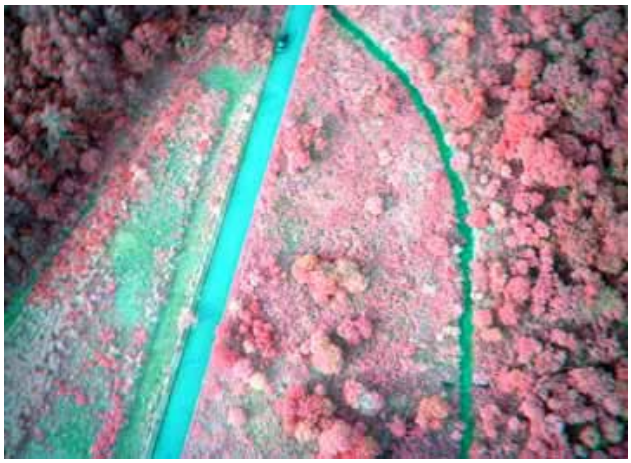

Fig. 14 False-Color Image

7.3 Orthomosaic Images

The original perspective aerial photographs contain image displacements caused by the tilting of cameras, in this case pitch and bank angles of the vehicle, and terrain relief. They don't have a uniform scale. Distances cannot be measured on the aerial photographs unlike in the case of maps. So, the photographs cannot be pieced into appropriate mosaic images, because scales are different from each other everywhere. The effects of tilt angle and relief are removed from the aerial photographs by a rectification process to create orthophotos. The orthophotos are uniform-scale photographs. It is a photographic map. Since an orthophoto has a uniform scale, it is possible to measure directly on it like other maps, and to piece each other into large orthomosaic images.

One of constructed orthomosaic images is shown in Fig.15. The rectification of relief wasn't processed, because a difference of elevation of the target area was not so large.

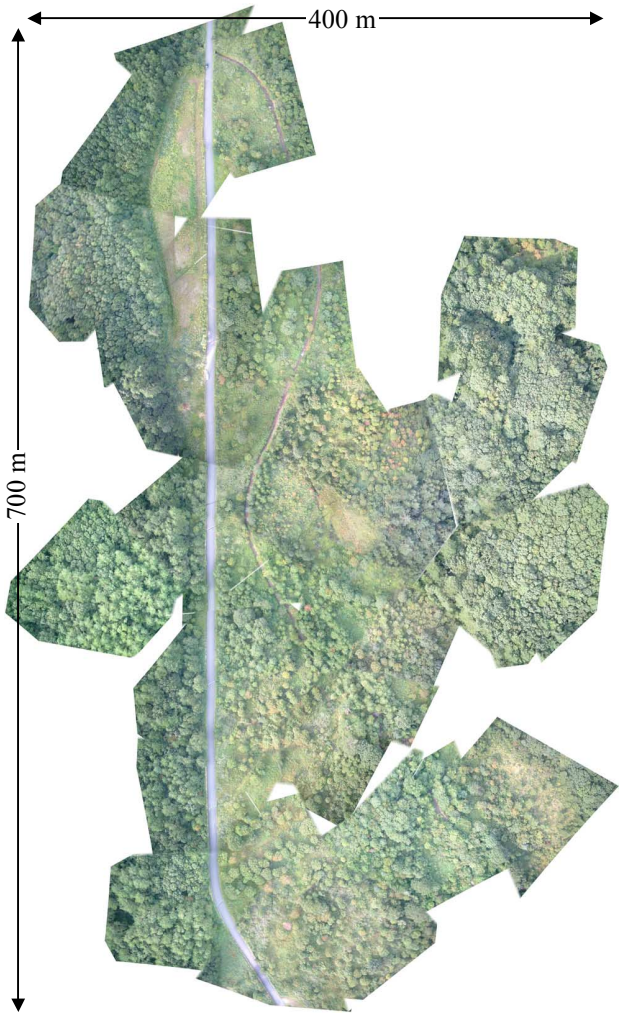

Fig. 15 Orthomosaic Image

7 Conclusion

Experimental small, no more than 1.5 m in the wingspans and 1.5 kg in the weights, 'one-person-portable' UAVs, OBK-SkyEye family were developed. SkyEye2 has demonstrated the feasibility of cellular phone data link system developed in this project. SkyEye3 was employed in aerial observation missions at forest area, Yahata moors, collaborating with the forestry research center. Collected photographs were processed into false-color images and orthomosaic images useful for analysis of vegetations.

Acknowledgements

The authors would like to thank Ohta business development consortium (OBK) and IARP members for all their help, and acknowledge the contributions of Mr. Norio Yuba, who developed the multi-bands digital camera unit.

Finally, note that OBK-SkyEye was developed through entrustment by New Energy and Industrial Technology Development Organization (NEDO).

References

[1] *Unmanned Aircraft Systems Roadmap 2005-2030*. United States Department of Defense, electronic document (http://www.acq.osd.mil/usd/Roadmap Final2.pdf), August 2005

[2] Loegering G. Global Hawk – A New Tool for Airborne Remote Sensing, *1st technical Conference and Workshop on Unmanned Aerospace Vehicles*, AIAA 2002-3458, May. 20-23, 2002, Portsmouth, Virginia.

[3] Fahey D.W, et al. The NOAA Unmanned Aerial System (UAS) Demonstration Project Using the General Atomics Altair UAS. *Infotech@Aerospace*, September 26-29 2005, Arlington, Virginia.

[4] Abershitz A, et al. IAI's Micro / Mini UAV Systems – Development Approach. *Infotech@Aerospace*, September 26-29 2005, Arlington, Virginia.

[5] Enderle B. Commercial applications of UAV's in Japanese Agriculture. *AIAA 1st UAV conference*, Portsmouth, Virginia, AIAA 2002-3400, 2002

[6] D. Kubo and S. Suzuki, Design, Build and Fly of Experimental Model-Airplane, *Proceedings of KSAS-JSASS Joint Symposium on Aerospace Engineering*, pp.247-251, Nov. 18-19, 2004, Seoul, Korea.

[7] CEMAP: http://www.flight.t.u-tokyo.ac.jp/soft/

[8] Rae W. H., Jr. and Pope A. *Low-Speed Wind Tunnel Testing*. A Wiley-Interscience Publication, New York / Chichester / Brisbane / Singapore, 1984

[9] Gessow A and Myers G. C., Jr. *Aerodynamics of the Helicopter*. *Journal Name*, The Macmillan Co., New York, 1952.

[10] AeroSim Blockset: Unmanned Dynamics, LLC http://www.u-dynamics.com/